Synthesis and Structure of the Novel 11-Vertex Rhenacarborane Dianion [1,1,1-(CO)$_3$-2-Ph-*closo*-1,2-ReCB$_9$H$_9$]$^{2-}$ and Its Reactivity toward Cationic Transition Metal Fragments

Shaowu Du, Jason A. Kautz, Thomas D. McGrath, and F. Gordon A. Stone*

Department of Chemistry & Biochemistry, Baylor University, Waco, Texas 76798-7348

Received February 21, 2003

Treatment of [NEt$_4$][6-Ph-*nido*-6-CB$_9$H$_{11}$] in tetrahydrofuran (THF) with Bu^{n}Li (2 equiv) followed by [ReBr(THF)$_2$(CO)$_3$] gives the title rhenacarborane dianion isolated, by addition of [N(PPh$_3$)$_2$]Cl, as a mixed salt [N(PPh$_3$)$_2$][NEt$_4$][1,1,1-(CO)$_3$-2-Ph-*closo*-1,2-ReCB$_9$H$_9$], whose structure was confirmed by X-ray diffraction. The *closo* 11-vertex dianion reacts readily with several cationic transition metal−ligand fragments, affording products with novel structures in which the electrophilic metal groups are attached exo-polyhedrally to the {*closo*-1,2-ReCB$_9$} cage system by rhenium−metal bonds supported by three-center two-electron B−H→M linkages. Species prepared include [1,3-{M(dppe)}-3-μ-H-1,1,1-(CO)$_3$-2-Ph-*closo*-1,2-ReCB$_9$H$_8$] (M = Ni, Pd, or Pt; dppe = Ph$_2$PCH$_2$CH$_2$PPh$_2$), [N(PPh$_3$)$_2$][1,3,6-{M(CO)$_3$}-3,6-(μ-H)$_2$-1,1,1-(CO)$_3$-2-Ph-*closo*-1,2-ReCB$_9$H$_7$] (M = Mn or Re), and [1,6-{M(PPh$_3$)}-1,7-{M(PPh$_3$)}-6,7-(μ-H)$_2$-1,1,1-(CO)$_3$-2-Ph-*closo*-1,2-ReCB$_9$H$_7$] (M = Cu or Au). Of these, the structures of the platinum−rhenium and dicopper−rhenium species were confirmed by X-ray diffraction.

Introduction

Although the first rhenacarborane, Cs[3,3,3-(CO)$_3$-*closo*-3,1,2-ReC$_2$B$_9$H$_{11}$] (**1**), was reported over 35 years ago by Hawthorne and co-workers,[1] until recently[2] its chemistry had been little studied.[3] The discovery of the rhenium monocarbollide species [N(PPh$_3$)$_2$]$_2$[2,2,2-(CO)$_3$-*closo*-2,1-ReCB$_{10}$H$_{11}$] (**2**)[4] and [1,2-μ-NHBu^t-2,2,2-(CO)$_3$-*closo*-2,1-ReCB$_{10}$H$_{10}$] (**3**)[5] with the demonstration that their chemistry is also extensive has greatly extended this area for research. The rhenacarborane anion of **1** and the dianion of **2** both react with a variety of cationic transition metal fragments to form bimetallic species. However, whereas the derivatives of **2** all contain direct metal−metal connectivities supported by additional three-center two-electron B−H→M bonds,[4,6] the anion of **1** affords both metal−metal bonded products and species in which the auxiliary metal fragment is attached to the rhenacarborane solely by B−H→M linkages.[2,7,8] This behavior of **2** contrasts with that of the corresponding—albeit monoanionic—molybdenum− and iron−monocarborane clusters which exclusively form bimetallic species without metal−metal bonds in the complexes reported to date.[9]

Seeking to extend these studies to other anionic metallacarboranes our attention was drawn to the recent report of a facile synthesis of the 10-vertex monocarborane monoanion [6-Ph-*nido*-6-CB$_9$H$_{11}$]$^-$.[10−12]

Chart 1

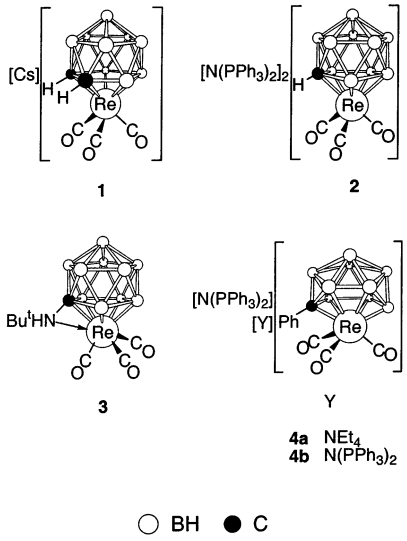

* To whom correspondence should be addressed. E-mail: gordon_stone@baylor.edu.

(1) Hawthorne, M. F.; Andrews, T. D. *J. Am. Chem. Soc.* **1965**, *87*, 2496. Hawthorne, M. F.; Young, D. C.; Andrews, T. D.; Howe, D. V.; Pilling, R. L.; Pitts, A. D.; Reintjes, M.; Warren, L. F., Jr.; Wegner, P. A. *J. Am. Chem. Soc.* **1968**, *90*, 879.

(2) Ellis, D. D.; Jelliss, P. A.; Stone, F. G. A. *Organometallics* **1999**, *18*, 4982.

(3) (a) Grimes, R. N. In *Comprehensive Organometallic Chemistry*; Wilkinson, G., Abel, E. W., Stone, F. G. A., Eds.; Pergamon Press: Oxford, U.K., 1982; Vol. 1, Section 5.5. (b) Grimes, R. N. In *Comprehensive Organometallic Chemistry II*; Abel, E. W., Stone, F. G. A., Wilkinson, G., Eds.; Pergamon Press: Oxford, U.K., 1995; Vol. 1, Chapter 9.

(4) Blandford, I.; Jeffery, J. C.; Jelliss, P. A.; Stone, F. G. A. *Organometallics* **1998**, *17*, 1402.

(5) Du, S.; Kautz, J. A.; McGrath, T. D.; Stone, F. G. A. *Chem. Commun.* **2002**, 1004.

(6) Jeffery, J. C.; Jelliss, P. A.; Rees, L. H.; Stone, F. G. A. *Organometallics* **1998**, *17*, 2258.

(7) Ellis, D. D.; Jelliss, P. A.; Stone, F. G. A. *J. Chem. Soc., Dalton Trans.* **2000**, 2113.

(8) Ellis, D. D.; Jeffery, J. C.; Jelliss, P. A.; Kautz, J. A.; Stone, F. G. A. *Inorg. Chem.* **2001**, *40*, 2041.

(9) Ellis, D. D.; Franken, A.; Jelliss, P. A.; Kautz, J. A.; Stone, F. G. A.; Yu, P.-Y. *J. Chem. Soc., Dalton Trans.* **2000**, 2509.

10.1021/om030122a CCC: $25.00
Publication on Web 05/31/2003

Table 1. Analytical and Physical Data

compd	color	yield/%	ν_{max}(CO)[a]/cm^{-1}	anal./%[b,c] C	anal./%[b,c] H
[N(PPh$_3$)$_2$][NEt$_4$][1,1,1-(CO)$_3$-2-Ph-*closo*-1,2-ReCB$_9$H$_9$] (**4a**)	yellow	89	1978 vs, 1888 s, 1852 s	57.4 (57.2)	5.9 (5.7)
[1,3-{Ni(dppe)}-3-μ-H-1,1,1-(CO)$_3$-2-Ph-*closo*-1,2-ReCB$_9$H$_8$] (**5**)	burgundy	36	2049 vs, 1988 w, 1959 m	46.6 (46.8)	4.0 (4.2)
[1,3-{Pd(dppe)}-3-μ-H-1,1,1-(CO)$_3$-2-Ph-*closo*-1,2-ReCB$_9$H$_8$] (**6**)	purple	79	2046 vs, 1986 w, 1952 m	44.7 (44.6)	3.9 (3.9)
[1,3-{Pt(dppe)}-3-μ-H-1,1,1-(CO)$_3$-2-Ph-*closo*-1,2-ReCB$_9$H$_8$] (**7a**)	orange-red	71	2048 vs, 1988 w, 1952 m	40.8 (40.8)	3.5 (3.6)
[1,3-{Pt(PPh$_3$)$_2$}-3-μ-H-1,1,1-(CO)$_3$-2-Ph-*closo*-1,2-ReCB$_9$H$_8$] (**7b**)	orange-red	55	2050 vs, 1997 w, 1963 m	45.5 (45.5)[d]	3.7 (3.7)
[N(PPh$_3$)$_2$][1,3,6-{Re(CO)$_3$}-3,6-(μ-H)$_2$-1,1,1-(CO)$_3$-2-Ph-*closo*-1,2-ReCB$_9$H$_7$] (**8**)	yellow	68	2051 s, 2021 vs, 1977 w, 1947 s, 1919 m	46.3 (46.2)	3.5 (3.5)
[N(PPh$_3$)$_2$][1,3,6-{Mn(CO)$_3$}-3,6-(μ-H)$_2$-1,1,1-(CO)$_3$-2-Ph-*closo*-1,2-ReCB$_9$H$_7$] (**9**)	burgundy	63	2050 s, 2017 vs, 1974 m, 1953 s, 1931 m	51.6 (51.5)	4.1 (3.9)
[1,6-{Cu(PPh$_3$)}-1,7-{Cu(PPh$_3$)}-6,7-(μ-H)$_2$-1,1,1-(CO)$_3$-2-Ph-*closo*-1,2-ReCB$_9$H$_7$] (**10a**)	yellow	55	2021 s, 1959 s, 1918 s	48.5 (48.2)[d]	3.9 (3.9)
[1,6-{Au(PPh$_3$)}-1,7-{Au(PPh$_3$)}-6,7-(μ-H)$_2$-1,1,1-(CO)$_3$-2-Ph-*closo*-1,2-ReCB$_9$H$_7$] (**11**)	yellow	43	2021 s, 1957 s, 1917 s	39.8 (39.9)	3.4 (3.2)

[a] Measured in CH_2Cl_2; the broad, medium-intensity band observed at ca. 2500−2550 cm^{-1} in the spectra of all compounds is due to B−H absorptions. [b] Calculated values are given in parentheses. [c] Analyses for N/%: **4a**, 2.4 (2.5); **8** 1.2 (1.2); **9** 1.3 (1.1). [d] Cocrystallizes with 0.5 molar equiv of CH_2Cl_2.

After double deprotonation the latter should afford the putative trianion [6-Ph-*nido*-6-CB$_9$H$_9$]$^{3-}$, formally comparable with the 11-vertex carborane ligand [*nido*-7-CB$_{10}$H$_{11}$]$^{3-}$ in **2**. Reactions of the trianion with electrophilic metal−ligand fragments should thus occur. However, whereas {*closo*-MCB$_{10}$} species contain a metal center that is *pentahapto*-coordinated by the carborane ligand, the corresponding {*closo*-MCB$_9$} compounds will contain a *hexahapto*-ligating carborane cage system. This, and the potential for other differences in structural behavior, prompted us to investigate as a promising entry point the 11-vertex rhenacarborane species. We here report the synthesis and characterization of the first non-icosahedral rhenium−carborane cluster and demonstrate its reactivity with a range of transition metal fragments.

Results and Discussion

The rhenacarborane anions of compounds **1** and **2** were prepared[2,4] in good yields by reaction of the anionic carborane ligands [*nido*-7,8-C$_2$B$_9$H$_{11}$]$^{2-}$ and [*nido*-7-CB$_{10}$H$_{11}$]$^{3-}$, respectively, with the rhenium synthon [ReBr(THF)$_2$(CO)$_3$].[13] Use of the latter afforded a considerably improved yield in the synthesis of **1**[2] and was thus the reagent of choice in the present work. Thus, treatment of [NEt$_4$][6-Ph-*nido*-6-CB$_9$H$_{11}$][10−12] with Bu^{n}Li (2 equiv) followed by [ReBr(THF)$_2$(CO)$_3$] gave the dianion [1,1,1-(CO)$_3$-2-Ph-*closo*-1,2-ReCB$_9$H$_9$]$^{2-}$, typically isolated as a mixture of the salts **4a** and **4b** by addition of [N(PPh$_3$)$_2$]Cl. The actual existence during the synthesis of the trianion [6-Ph-*nido*-6-CB$_9$H$_9$]$^{3-}$, either in solution or as a precipitate, is only inferred; no attempt was made to isolate or identify such a species. The corresponding 11-vertex trianion [*nido*-7-CB$_{10}$H$_{11}$]$^{3-}$, as the trisodium salt, forms as a copious white precipitate in THF,[14] but no similar solid was observed in the present work. Nevertheless, the [6-Ph-*nido*-6-CB$_9$H$_9$]$^{3-}$ trianion can be reasonably invoked and is certainly found coordinated to the Re^I center in the product **4**.

Complete metathesis of the product mixture to the salt **4b** could not be achieved, even employing a large excess of [N(PPh$_3$)$_2$]Cl. However, pure samples of **4a** were obtained by fractional crystallization of the mixture of **4a** and **4b**, and the species was characterized by the data given in Tables 1−3. In its ^{11}B{^{1}H} NMR spectrum the rhenacarborane dianion gives rise to five signals between δ 32.3 and −29.1 in the ratio 1:1:3:2:2, consistent with the expected mirror-symmetric {*closo*-1,2-ReCB$_9$} cluster architecture, with the peak of relative intensity 3 arising from a coincidence. A characteristic broad resonance at δ 52.9 is seen in its ^{13}C{^{1}H} NMR spectrum, corresponding to the cage-carbon atom, and peaks attributable to the cage-phenyl group and to the cations are also seen in typical positions in the ^{1}H and ^{13}C{^{1}H} NMR spectra. Interestingly, the resonance for the *ipso* carbon atom of the carborane-bound phenyl ring occurs to relatively high frequency, at δ 156.6.

Although the structure of the rhenacarborane anion in **4** was reasonably substantiated by the spectroscopic data, further confirmation was provided by an X-ray diffraction study on **4a**, which revealed the structure shown in Figure 1. This established unequivocally that the cluster moiety consists of an {Re(CO)$_3$} fragment that is η^6-coordinated by the CBBBBB face of the {6-Ph-*nido*-6-CB$_9$H$_9$} ligand. The rhenium vertex is considerably closer to the two "prow" atoms of the boat-shaped ligating face, with Re−C(1) 2.226(8) Å and Re−B(4) 2.210(12) Å, than to the other four coordinating boron atoms (Re−B range 2.477(11)−2.525(10) Å), a feature typical of such *closo*-11-vertex 1-metalla(hetero)-boranes.[15,16] We believe **4** to be the first non-icosahedral rhenacarborane cluster and also the first reported metal

(10) Brellochs, B. In *Contemporary Boron Chemistry*; Davidson, M. G., Hughes, A. K., Marder, T. B., Wade, K., Eds.; Royal Soc. Chem., Cambridge, U.K., 2000; p 212.
(11) Jelínek, T.; Kilner, C. A.; Thornton-Pett, M.; Kennedy, J. D. *Chem. Commun.* **2001**, 1790.
(12) Jelínek, T.; Thornton-Pett, M.; Kennedy, J. D. *Collect. Czech. Chem. Commun.* **2002**, *67*, 1035.
(13) Vitali, D.; Calderazzo, F. *Gazz. Chim. Ital.* **1972**, *102*, 587.
(14) Hyatt, D. E.; Scholer, F. R.; Todd, L. J.; Warner, J. L. *Inorg. Chem.* **1967**, *6*, 2229.
(15) Kennedy, J. D. *Prog. Inorg. Chem.* **1986**, *34*, 211.

Table 2. ^{1}H and ^{13}C NMR Data[a]

	^{1}H/δ [b]	^{13}C/δ [c]
4a	7.97 (d, ^{3}J(HH) = 8, 2H, cage-C$_6H_5$ (*ortho*)), 7.69−7.44 (m, 30H, PPh), 7.10 (dd, ^{3}J(HH) = ^{3}J(HH) = 8, 2H, cage-C$_6H_5$ (*meta*)), 6.88 (t, 1H, cage-C$_6H_5$ (*para*)), 3.24 (q, J(HH) = 7, 8H, NCH$_2$), 1.26 (t, 12H, CH$_3$)	199.8 (CO), 156.6 (cage-*C*$_6$H$_5$ (*ipso*)), 134.1−126.7 (PPh), 129.8 (cage-*C*$_6$H$_5$ (*ortho*)), 126.8 (cage-*C*$_6$H$_5$ (*meta*)), 122.6 (cage-*C*$_6$H$_5$ (*para*)), 68.0 (NCH$_2$), 52.9 (br, cage C), 7.8 (CH$_3$)
5	7.69 (d, ^{3}J(HH) = 8, 2H, cage-C$_6H_5$ (*ortho*)), 7.69−7.44 (vbr m, 20H, PPh), 7.27 (dd, ^{3}J(HH) = ^{3}J(HH) = 8, 2H, cage-C$_6H_5$ (*meta*)), 7.16 (t, 1H, cage-C$_6H_5$ (*para*)), 2.32, 2.03 (br m × 2, 2H × 2, CH$_2$ × 2)	189.7 (vbr, CO), 149.5, 134.9−126.7 (Ph), 98.6 (br, cage C), 27.8 (vbr, CH$_2$)
6	7.69 (d, ^{3}J(HH) = 8, 2H, cage-C$_6H_5$ (*ortho*)), 7.61−7.49 (m, 20H, PPh), 7.28 (dd, ^{3}J(HH) = ^{3}J(HH) = 8, 2H, cage-C$_6H_5$ (*meta*)), 7.17 (t, 1H, cage-C$_6H_5$ (*para*)), 2.60, 2.47 (br m × 2, 2H × 2, CH$_2$)	189.9 (br, CO), 150.1, 134.3−126.6 (Ph), 102.0 (br, cage C), 30.1, 26.4 (br × 2, CH$_2$ × 2)
7a	7.72−7.54 (m, 22H, cage-C$_6H_5$ (*ortho*) and PPh), 7.27 (dd, ^{3}J(HH) = ^{3}J(HH) = 8, 2H, cage-C$_6H_5$ (*meta*)), 7.15 (t, 2H, cage-C$_6H_5$ (*para*)), ca. 2.3 (vbr, 4H, CH$_2$)	189.8 (CO, J(PtC) = 22), 149.6, 132.7−126.5 (Ph), 92.8 (br, cage C), 28.3 (br, CH$_2$)
7b	7.75−7.13 (m, 35H, Ph)	193.1 (CO, J(PtC) = ca. 25),[d] 149.0, 134.7−125.3 (Ph)
8	7.86 (d, ^{3}J(HH) = 7, 2H, cage-C$_6H_5$ (*ortho*)), 7.69−7.45 (m, 30H, PPh) 7.30 (dd, ^{3}J(HH) = ^{3}J(HH) = 7, 2H, cage-C$_6H_5$ (*meta*)), 7.15 (t, 1H, cage-C$_6H_5$ (*para*)), ca. −3.5 (br q, J(BH) = ca. 120, B−H⇀Re), ca. −7.9 (br q, J(BH) = ca. 100, B−H⇀Re)	197.6, 195.4, 192.7, 189.8, 189.7, 187.3 (CO × 6), 151.1, 135.0−125.7 (Ph), 63.5 (br, cage C)
9[e]	7.87 (br, 2 H, cage-C$_6H_5$ (*ortho*)), 7.63−7.44 (m, 30H, PPh), 7.26 (br, 2H, cage-C$_6H_5$ (*meta*)), 7.13 (br, 1H, cage-C$_6H_5$ (*para*)), ca. −5.2, ca. −9.6 (br m × 2, B−H⇀Mn × 2)	224.5, 223.8, 222.8 (br × 3, Mn−CO × 3), 190.5, 188.8, 186.6 (Re−CO × 3), 150.5, 135.7−125.1 (Ph), 62.6 (br, cage C)
10a	7.89 (dd, ^{3}J(HH) = 8, ^{4}J(HH) = 1, 2H, cage-C$_6H_5$ (*ortho*)), 7.55−7.42 (m, 30H, Ph), 7.32 (dd, ^{3}J(HH) = ^{3}J(HH) = 8, 2H, cage-C$_6H_5$ (*meta*)), 7.18 (tt, 1H, cage-C$_6H_5$ (*para*))	190.4 (br, CO), 186.7 (br, 2 × CO), 149.3, 136.4−126.1 (Ph), 59.3 (br, cage C)
10b	7.85 (dd, ^{3}J(HH) = 8, ^{4}J(HH) = 1, 2H, cage-C$_6H_5$ (*ortho*)), 7.29 (dd, ^{3}J(HH) = ^{3}J(HH) = 8, 2H, cage-C$_6H_5$ (*meta*)), 7.15 (tt, 1H, cage-C$_6H_5$ (*para*)), 2.34 (s, 6H, Me)	189.9 (br, CO), 186.2 (br, 2 × CO), 149.4, 128.6, 128.3, 125.9 (Ph), 118.9 (C≡N) 57.8 (br, cage C), 3.2 (Me)
11	7.85 (dd, ^{3}J(HH) = 8, ^{4}J(HH) = 1, 2H, cage-C$_6H_5$ (*ortho*)), 7.57−7.44 (m, 30H, Ph), 7.26 (dd, ^{3}J(HH) = ^{3}J(HH) = 8, 2H, cage-C$_6H_5$ (*meta*)), 7.12 (tt, 1H, cage-C$_6H_5$ (*para*))	191.1 (CO), 188.1 (vbr, 2 × CO), 148.7, 136.7−125.8 (Ph), 54.9 (br, cage C)

[a] Chemical shifts (δ) in ppm, coupling constants (J) in hertz; measurements at ambient temperatures, except where indicated, in CD_2Cl_2. [b] Resonances for terminal BH protons occur as broad unresolved signals in the range δ ca. −1 to +3. [c] ^{1}H-decoupled chemical shifts are positive to high frequency of $SiMe_4$. [d] The resonance for the cage-carbon atom was not observed: the spectrum is weak as a result of poor solubility of the product. [e] Measured at 210 K.

complex of the [6-Ph-*nido*-6-CB$_9$H$_9$]$^{3-}$ carborane ligand. Its straightforward synthesis in good yield made it an ideal substrate for further studies, the initial results of which are presented below.

As was the case with compound **2**,[4,6] it seemed reasonable that the dianion of **4** would combine with dicationic metal fragments to give neutral bimetallic species. However, in contrast to the {ReCB$_{10}$} system,[6] reaction of **4** with the dication [Rh(NCMe)$_3$(η^5-C$_5$Me$_5$)]$^{2+}$ has so far failed to afford any tractable products. Instead it appears that additional redox reactions occurred,[17,18] leading to a number of as yet unidentified, possibly polymetallic species.

Treatment of **4** with nickel−, palladium−, and platinum−phosphine fragments proved more successful. With the complexes [MCl$_2$(dppe)] (dppe = Ph$_2$PCH$_2$CH$_2$PPh$_2$), in the presence of Tl[PF$_6$] (2 equiv) to remove Cl$^-$ as insoluble TlCl, the neutral products [1,3-{M(dppe)}-3-μ-H-1,1,1-(CO)$_3$-2-Ph-*closo*-1,2-ReCB$_9$H$_8$] (M = Ni (**5**); Pd (**6**); Pt (**7a**)) were obtained. The related species [1,3-{Pt(PPh$_3$)$_2$}-3-μ-H-1,1,1-(CO)$_3$-2-Ph-*closo*-1,2-ReCB$_9$H$_8$] (**7b**) was prepared similarly. In structural formulas, for the purposes of assigning suitable electron counts to the metal centers, these molecules may be represented as either **A**, **B**, or **C** (Figure 2). Note that all three are canonical forms and that, as with all cluster compounds, precise electron distributions cannot definitively be assigned. Thus, although the metal−metal bonds as shown in the charts and schemes are drawn

Table 3. ^{11}B and ^{31}P NMR Data[a]

	^{11}B/δ [b]	^{31}P/δ [c]
4a	32.3, 8.7, −7.7 (3B), −27.4 (2B), −29.1 (2B)	21.7
5	21.0, 12.4, 9.9, 7.0, −8.0, −12.8, −14.5, −15.5, −18.3	55.5 (br)
6[d]	20.9, 18.1, 7.6 (2B), −8.2, −10.8, −13.0, −14.6, −16.7	52.3 (br), 47.9 (br)
7a[d]	18.1, 13.1, 7.3, 5.1, −10.0, −12.8, −15.9 (2B), −20.0	53.5 (J(PtP) = 3809)
7b[d]	20.5, 14.9, 5.6 (2B), −11.9 (5B)	19.4 (J(PtP) = 4055)
8	19.1, 14.6, 5.3, −12.2 (2B), −17.4, −22.5, −23.9, −29.2	21.7
9	20.4, 15.3, 5.1, −11.5 (2B), −17.1, −23.7 (2B), −28.8	21.7
10a	7.3 (2B), 3.1, −9.3 (2B), −26.4 (2B), −30.8 (2B)	10.1 (br)
10b	5.5, 2.6, 1.3, −9.0 (2B), −27.6 (2B), −35.7 (2B)	
11	17.7, 5.4, −0.6, −7.7 (2B), −25.0 (2B), −28.4 (2B)	40.7

[a] Chemical shifts (δ) in ppm, coupling constants (J) in hertz; measurements at ambient temperatures in CD_2Cl_2. [b] ^{1}H-decoupled chemical shifts are positive to high frequency of BF_3·Et_2O (external); resonances are of unit integral except where indicated. [c] ^{1}H-decoupled chemical shifts are positive to high frequency of 85% H_3PO_4 (external). [d] Peak integrals' assignments may be somewhat subjective, and some coupling information could not be resolved, because spectra are weak as a result of the poor solubility of the product.

(16) Barton, L.; Srivastava, D. K. In *Comprehensive Organometallic Chemistry II*; Abel, E. W., Stone, F. G. A., Wilkinson, G., Eds.; Pergamon Press: Oxford, U.K., 1995; Vol. 1, Chapter 8.
(17) Mullica, D. F.; Sappenfield, E. L.; Stone, F. G. A.; Woollam, S. F. *J. Chem. Soc., Dalton Trans.* **1993**, 3559.
(18) Du, S.; Kautz, J. A.; McGrath, T. D.; Stone, F. G. A. *Inorg. Chem.* **2002**, *41*, 3202.

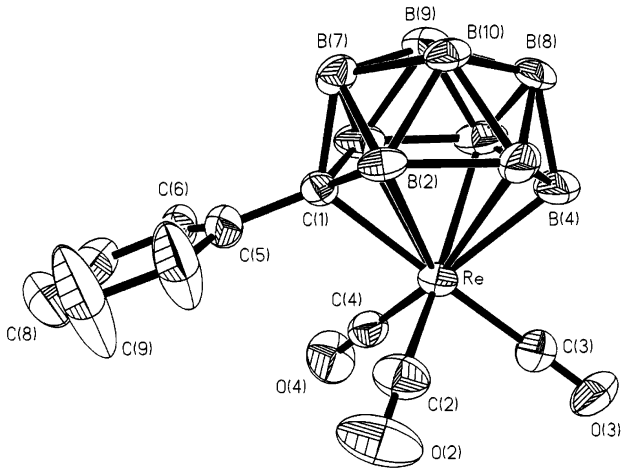

Figure 1. Structure of the dianion of **4a** showing the crystallographic labeling scheme. Hydrogen atoms are omitted for clarity, and thermal ellipsoids are drawn with 40% probability. Selected distances (Å) and angles (deg): Re−C(1) 2.226(8), Re−B(2) 2.525(10), Re−B(3) 2.492(11), Re−B(4) 2.210(12), Re−B(5) 2.477(11), Re−B(6) 2.512(11), Re−C(2) 1.915(12), C(2)−O(2) 1.147(12), Re−C(3) 1.904(11), C(3)−O(3) 1.173(11), Re−C(4) 1.930(12), C(4)−O(4) 1.158(11), C(1)−C(5) 1.490(12), C(1)−B(2) 1.599(13), C(1)−B(6) 1.575(14), B(2)−B(3) 1.895(16), B(3)−B(4) 1.725(19), B(4)−B(5) 1.657(18), B(5)−B(6) 1.868(17); C(2)−Re−C(1) 92.8(4), C(3)−Re−C(1) 177.0(4), C(4)−Re−C(1) 89.7(3), O(2)−C(2)−Re 178.6(11), O(3)−C(3)−Re 179.0(7), O(4)−C(4)−Re 179.2(9), Re−C(1)−C(5) 120.3(6), B(6)−C(1)−B(2) 110.5(8), C(1)−B(2)−B(3) 118.1(8), B(4)−B(3)−B(2) 119.7(9), B(5)−B(4)−B(3) 102.8(9), B(4)−B(5)−B(6) 122.1(9), C(1)−B(6)−B(5) 118.6(9).

Chart 2

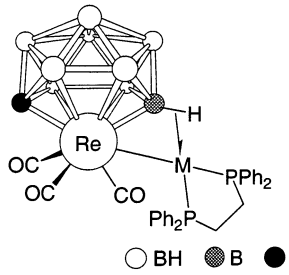

	M
5	Ni
6	Pd
7a	Pt

○ BH ◍ B ● CPh

for simplicity as a single line, this need not imply a conventional single bond. This depiction is used only to indicate the presence of a connectivity and does not necessarily denote a particular distribution of electrons. A similar treatment is applied to compounds **8**−**11** discussed later.

Compounds **5**−**7** were characterized spectroscopically and, in addition, compound **7a** was studied by X-ray diffraction methods. The results of the structure determination are discussed first, as they are relevant to consideration of the NMR data. Two views of a molecule of **7a** are presented in Figure 3. A {Pt(dppe)} fragment is seen to be located at a site exo-polyhedral to the rhenacarborane cluster, bonded via a Re−Pt linkage (Re−Pt is 2.7473(5) Å) and a B−H⇀Pt three-center, two-electron agostic-type bond (B(4)−Pt 2.266(11), Pt−H(4) 2.04(11), B(4)−H(4) 1.07(10) Å). The platinum fragment {$Pt(PPh_3)_2$} in the corresponding derivative of compound **2** is similarly attached to the cluster but, perhaps significantly, with a more intimate B−H⇀Pt interaction (B−Pt 2.355(3), Pt−H 1.57(4), B−H 1.37(4) Å) and a slightly longer Re−Pt bond (2.7931(4) Å).[4] However, although the schematic representation of compounds **5**−**7** and the perspective in Figure 3a might suggest that the Re−M and B−H⇀M units lie close to the notional mirror plane (through C(1), Re, and B(4)) of the rhenacarborane subunit, Figure 3b shows that this is clearly not the case. Indeed, it is also apparent that the platinum center lies close to both B(3) and C(2) (Pt···B(3) is 2.499(10) Å and Pt···C(2) is 2.557(9) Å). This results in a Pt···H(3) contact that is relatively close but, at over 2.3 Å, would be a minimal interaction. Similarly, the close approach of C(2) to the platinum is likely responsible for the slight deviation from linearity of the Re−C(2)−O(2) angle (171.6(8)°), but this effect is relatively small.

Spectroscopic and other characterizing data for compounds **5**−**7** are given in Tables 1−3. All show resonances in the expected ranges in their ^{1}H and ^{13}C{^{1}H} NMR spectra for the phosphine ligands and the cage-phenyl groups. However, no signals are seen in the ^{1}H NMR spectra that may be attributed to protons involved in the three-center B−H⇀M linkages supporting the exo-polyhedral metal fragment. This is believed to be a consequence of dynamic behavior which is fast on the NMR time scale,[9] discussed below. In addition, the cage C atom appears as a broad peak at around δ 100 in the ^{13}C{^{1}H} NMR spectra, significantly to higher frequency than in the precursor **4**. The reason for this rather large downfield shift (ca. 40−50 ppm) is not clear. However, it is noteworthy that only a relatively small deshielding (ca. 10 ppm) is observed in the corresponding Pt and Pd derivatives of **2**.[4] In the carbonyl region of the ^{13}C{^{1}H} NMR spectra, the signal due to the rhenium-bound carbonyl ligands is a single, rather broad peak at around δ 190 with, for compounds **7**, apparent satellites due to weak coupling with the ^{195}Pt isotope (J(PtC) is ca. 25 Hz). In the ^{11}B{^{1}H} NMR spectra, the absence of molecular mirror symmetry is immediately apparent. Thus, the spectrum of **5** shows nine separate reso-

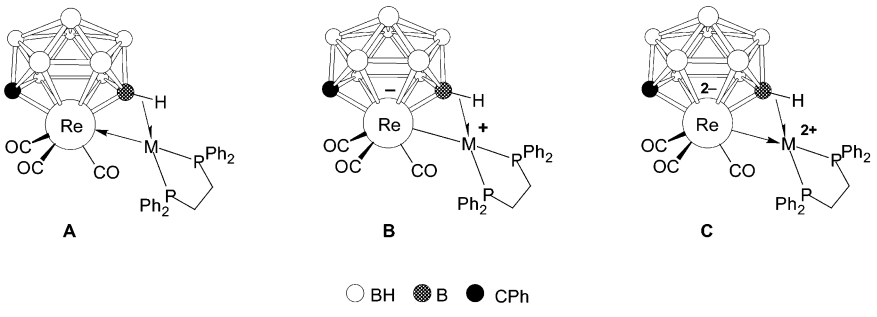

Figure 2. Three different canonical forms of compounds **5**−**7**.

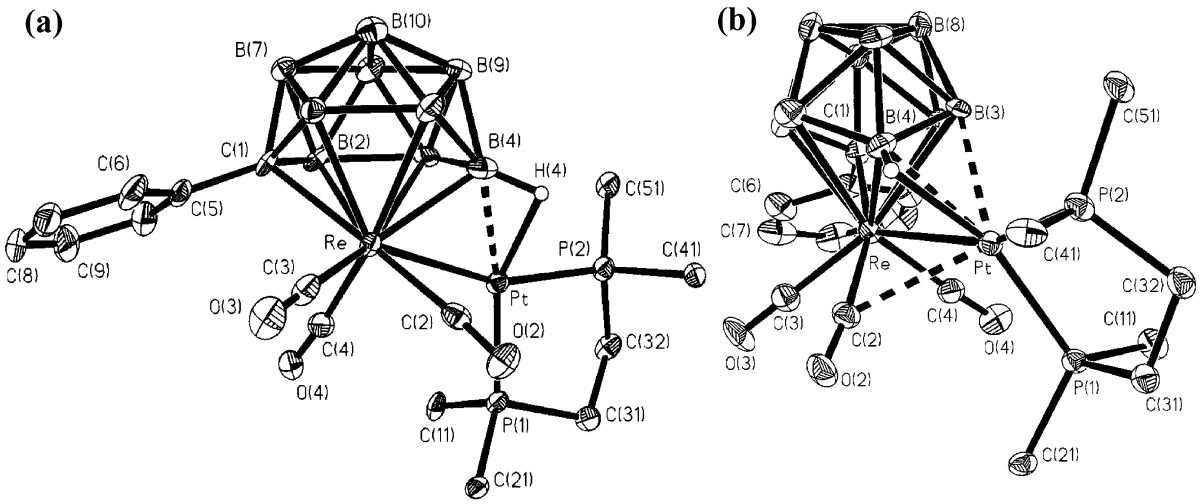

Figure 3. Two views of the molecular structure of **7a** showing the crystallographic labeling scheme: (a) a general perspective; and (b) a view emphasizing the platinum coordination environment. All but the *ipso* carbon atoms of phosphine phenyl rings, and all hydrogen atoms except H(4), are omitted for clarity; thermal ellipsoids are drawn at the 40% probability level. Selected distances (Å) and angles (deg): Re−C(1) 2.210(8), Re−B(2) 2.454(9), Re−B(3) 2.547(9), Re−B(4) 2.258(12), Re−B(5) 2.482(11), Re−B(6) 2.437(10), Re−Pt 2.7473(5), Re−C(2) 1.967(9), C(2)−O(2) 1.158(10), Re−C(3) 1.980(10), C(3)−O(3) 1.122(11), Re−C(4) 1.960(10), C(4)−O(4) 1.137(11), B(4)−Pt 2.266(11), B(4)−H(4) 1.07(10), H(4)−Pt 2.04(11), C(2)···Pt 2.557(9), B(3)···Pt 2.499(10); C(4)−Re−C(2) 99.0(4), C(4)−Re−C(3) 90.1(4), C(2)−Re−C(3) 79.2(4), C(4)−Re−Pt 81.7(3), C(2)−Re−Pt 63.2(3), C(3)−Re−Pt 139.4(2), C(1)−Re-Pt 132.9(2), B(4)−Re−Pt 52.7(3), Re−B(4)−Pt 74.8(3), O(2)−C(2)−Re 171.6(8), O(2)−C(2)−Pt 115.0(7), O(3)−C(3)−Re 178.2(8), O(4)−C(4)−Re 175.2(8), P(1)−Pt−B(4) 166.1(3), P(2)−Pt−B(4) 107.3(3), P(1)−Pt−Re 115.64(6), P(2)−Pt−Re 159.62(6), B(4)−Pt−Re 52.5(3).

Scheme 1. Proposed Behavior of Compounds 5−7 in Solution

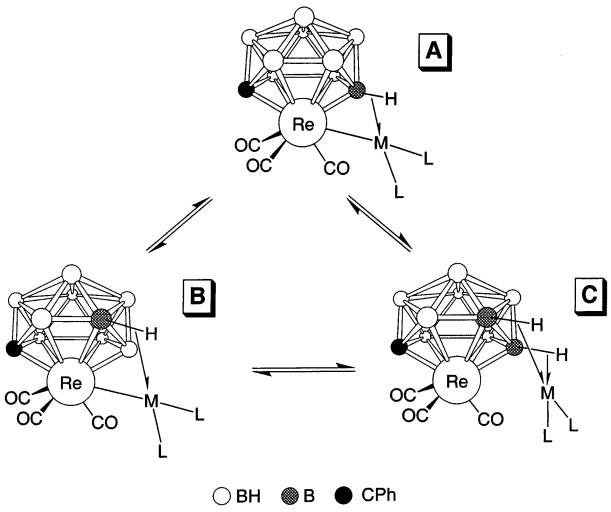

nances, while those for **6** and **7a** both show eight signals, of which one in each case is of relative intensity 2 due to a coincidence. (Poor solubility renders the spectrum of **7b** so broad that such conclusions cannot reliably be made.)

Although molecular asymmetry in solution is consistent with a static structure such as that observed in the solid state for **7a**, this cannot be reconciled with all of the NMR data. Thus it is thought that in solution the compounds interconvert between several structures, such as those shown in Scheme 1. In particular, the $^{31}P\{^1H\}$ NMR spectra of compounds **5** and **7** show only a single resonance, with characteristic ^{195}Pt satellites for **7**. This would require at the very least an "in-place" rotation of the $\{M(PR_3)_2\}$ fragment with respect to the rhenacarborane cluster to render the two phosphorus atoms chemically equivalent. Interconversion of species **A**, **B**, and **C** (Scheme 1), for example, is equivalent to such a rotation over a $\{ReB_2\}$ face that is itself an asymmetric site. Moreover, since the three rhenium-bound CO ligands appear to be equivalent, it may be suggested that the $\{Re(CO)_3\}$ moiety also rotates with respect to the carborane ligand. The latter motion likely requires a breaking of the Re−M bond (e.g., **C** in Scheme 1), but the observation of ^{195}Pt satellites for the carbonyl groups in **7** equally implies a contribution of metal−metal bonded species such as **A** and **B**. Note that the absence of molecular symmetry implied by $^{11}B\{^1H\}$ NMR spectroscopy suggests that in any given molecule the exo-polyhedral moiety must remain to one side of the notional mirror plane through the central $\{ReCB_9\}$ cluster. Thus chiral **A** can interconvert with **B** and **C** as in Scheme 1, but although their respective mirror images **A′**, **B′**, and **C′** also mutually interconvert, they do not convert to **A**, **B**, and **C**. The compounds as-made, of course, occur as the racemates.

Although stable and neutral bimetallic complexes were obtained from interaction of the dianion of **4** with dicationic transition metal fragments, it was recognized that an even more intriguing possibility was treatment of **4** with *two* molar equivalents of a metal−ligand *mono*cation, which should give rise to trimetallic species. Indeed, it seemed reasonable that stepwise addition of two different metal fragments might be used to construct heterotrimetallic species supported by the carborane cage.

With this ultimate goal in mind, the reactivity of compound **4** was first explored with sources of the cations $\{M(CO)_3\}^+$ (M = Re, Mn), namely, $[ReBr(THF)_2(CO)_3]$ in the presence of $Tl[PF_6]$, and $[Mn(NCMe)_3(CO)_3][PF_6]$, in an attempt to form bimetallic species that still retain a single anionic charge for further reaction. The products obtained, $[N(PPh_3)_2][1,3,6\text{-}\{M(CO)_3\}\text{-}3,6\text{-}(\mu\text{-}H)_2\text{-}1,1,1\text{-}(CO)_3\text{-}2\text{-}Ph\text{-}closo\text{-}1,2\text{-}ReCB_9H_7]$ (M = Re (**8**) and

Chart 3

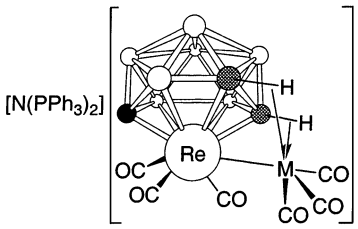

M

8 Re
9 Mn

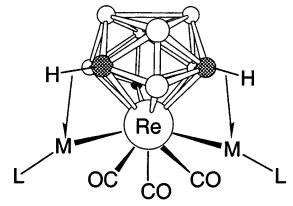

	M	L
10a	Cu	PPh_3
10b	Cu	NCMe
11	Au	PPh_3

○ BH ◍ B ● CPh

Mn (**9**), respectively), are characterized by the data given in Tables 1−3. Although crystals suitable for X-ray diffraction analysis could not be obtained, their structures are reasonably proposed to be as shown. The exo-polyhedral $\{M(CO)_3\}$ moiety in both **8** and **9** is bonded to the cluster via two nonequivalent three-center B−H→M interactions, with an Re−M bond completing the coordination sphere of the conical fragment. Broad quartet resonances for the protons involved in the agostic-type bridges are seen in the ^{1}H NMR spectra at δ ca. −3.5 and −7.9 for **8** and δ ca. −5.2 and −9.6 for **9**. In their $^{11}B\{^1H\}$ NMR spectra molecular asymmetry is evident, as there are seen to be nine inequivalent boron atoms (some resonances are accidentally coincident). Likewise, their $^{13}C\{^1H\}$ NMR spectra each reveal six separate resonances for the six carbonyl ligands. At ambient temperatures, however, those of the exo-polyhedral $\{Mn(CO)_3\}$ fragment in **9** appear as one broad signal, which separates into three peaks upon cooling to 210 K. This may be attributed to in-place rotation of the manganese moiety with respect to the cage that is arrested at the lower temperature, while the exo-polyhedral rhenium fragment in **8** is already static at room temperature. The cage-carbon atoms in **8** and **9** resonate at δ 63.5 and 62.6, respectively, to much lower frequency than in **5**−**7**, and rather closer to the expected range for *closo* metallacarboranes.[19]

Interestingly, treatment of **4** with excess of the rhenium or manganese reagents does not afford neutral, trimetallic species and only **8** or **9**, respectively, is isolated. This may be rationalized in terms of the proposed structure shown. In **8** and **9** the two B−H→M bridges that support the exo-polyhedral fragment are thought to involve β- and γ-BH vertexes in the CB*B*BB"belt" that η^6-ligates rhenium. This is consistent with the observed molecular asymmetry implied by the NMR data and with the known structure of **7a** described above. We have also observed generally for 12-vertex metal−monocarborane anions, in their reactions with metal cations[4,6,9] and with hydride abstracting reagents in the presence of donor molecules,[20−22] that within the metal-bound CBBBB ring it is the B−H units most distant from the cage-carbon atom that are the most hydridic. Thus in **8** and **9** a second exo-polyhedral $\{M(CO)_3\}$ unit cannot be accommodated since in the {*closo*-1,2-$ReCB_9$} framework there is only one γ-BH site, which in **8** and **9** is already occupied. Apparently alternative sites such as those involving α- and β-BH vertexes of the CB_5 face are not sufficiently attractive to an incoming second metal fragment. Indeed, the precise electronic structures of these anions may be such that interaction with such fragments is somehow "switched off". In this connection, it is notable that **8** and **9** also appeared not to react with cations such as $\{Cu(PPh_3)\}^+$ or $\{Au(PPh_3)\}^+$, which can be much less demanding in their coordination requirements.

These last observations on the reactivity of **8** and **9** provide an interesting contrast with the results of the direct reaction of the dianion of **4** with the same cationic copper or gold fragments. When compound **4** is treated with 1 equiv of $\{Cu(PPh_3)\}^+$ or $\{Au(PPh_3)\}^+$, derived from $[CuCl(PPh_3)]_4$ or $[AuCl(PPh_3)]$, respectively, in the presence of $Tl[PF_6]$, the sole products isolated in only modest yields are the neutral trimetal species [1,6-{M-(PPh_3)}-1,7-{M(PPh_3)}-6,7-(μ-H)$_2$-1,1,1-$(CO)_3$-2-Ph-*closo*-1,2-$ReCB_9H_7$] (M = Cu (**10a**), Au (**11**), respectively). The yields of these species are significantly improved, as might be expected, when two or more equivalents of $\{M(PPh_3)\}^+$ are employed. When **4** was treated similarly with the reagent $[Cu(NCMe)_4][PF_6]$, the related product [1,6-{Cu(NCMe)}-1,7-{Cu(NCMe)}-6,7-(μ-H)$_2$-1,1,1-$(CO)_3$-2-Ph-*closo*-1,2-$ReCB_9H_7$] (**10b**) was obtained. Unfortunately this product was unstable and, despite repeated attempts, failed to give satisfactory microanalytical or mass spectrometric data. It thus was not isolated for full characterization. The NCMe molecule was not displaced by another rhenacarborane cage to form a supramolecular cage species;[8] evidently **10b** exists as discrete molecules. Its potential for reaction, for example, with polydentate ligands, to form oligomeric species via NCMe displacement, is yet to be explored.

Data characterizing compounds **10** and **11** are given in Tables 1−3. However, their detailed structures were only established following an X-ray diffraction study upon a single crystal of **10a**, the results of which are discussed first. A preliminary (heavy-atom) structure determination upon compound **11** revealed it to have a comparable solid-state architecture, as would be expected. A perspective view of a molecule of **10a** is given in Figure 4, along with selected geometric parameters. Overall, the complex possesses approximate mirror symmetry and is seen to consist of a central rhenacarborane moiety, with two $\{Cu(PPh_3)\}$ fragments each

(19) For example: Brew, S. A.; Stone, F. G. A. *Adv. Organomet. Chem.* **1993**, *35*, 135.

(20) Ellis, D. D.; Franken, A.; Jelliss, P. A.; Stone, F. G. A.; Yu, P.-Y. *Organometallics* **2000**, *19*, 1993.

(21) Franken, A.; Du, S.; Jelliss, P. A.; Kautz, J. A.; Stone, F. G. A.; Yu, P.-Y. *Organometallics* **2001**, *20*, 1597.

(22) Du, S.; Franken, A.; Jelliss, P. A.; Kautz, J. A.; Stone, F. G. A.; Yu, P.-Y. *J. Chem. Soc., Dalton Trans.* **2001**, 1846.

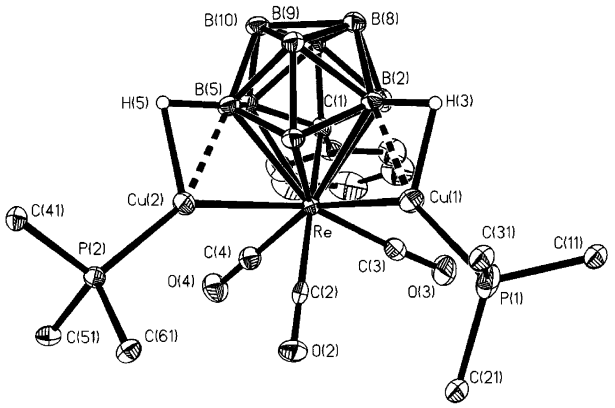

Figure 4. Structure of **10a** showing the crystallographic labeling scheme. All but the *ipso* carbon atoms of phosphine phenyl rings, and all hydrogen atoms except H(3) and H(5), are omitted for clarity. Thermal ellipsoids are drawn with 40% probability. Selected distances (Å) and angles (deg): Re−C(1) 2.251(5), Re−B(2) 2.531(6), Re−B(3) 2.502(6), Re−B(4) 2.266(6), Re−B(5) 2.503(6), Re−B(6) 2.524(5), Re−Cu(1) 2.7563(8), Re−Cu(2) 2.7866(7), Re−C(2) 1.945(5), C(2)−O(2) 1.153(6), Re−C(3) 1.952(6), C(3)−O(3) 1.133(7), Re−C(4) 1.955(6), C(4)−O(4) 1.141(6), B(3)−H(3) 1.21(5), B(3)−Cu(1) 2.095(5), Cu(1)−H(3) 1.82(5), B(5)−H(5) 1.22(5), B(5)−Cu(2) 2.096(6), Cu(2)−H(5) 1.95(5), Cu(1)−P(1) 2.194(2), Cu(2)−P(2) 2.1942(14); C(2)−Re−Cu(1) 68.7(2), C(3)−Re−Cu(1) 76.2(2), C(4)−Re−Cu(1) 150.4(2), B(3)−Re−Cu(1) 46.64(13), C(2)−Re−Cu(2) 65.9(2), C(3)−Re−Cu(2) 153.3(2), C(4)−Re−Cu(2) 82.6(2), B(5)−Re−Cu(2) 46.30(13), Cu(1)−Re−Cu(2) 93.89(2), B(3)−H(3)−Cu(1) 85(3), B(5)−H(5)−Cu(2) 79(3), Cu(1)−B(3)−Re 73.1(2), Cu(2)−B(5)−Re 74.0(2), O(2)−C(2)−Re 173.6(5), O(3)−C(3)−Re 176.7(5), O(4)−C(4)−Re 178.2(4), P(1)−Cu(1)−Re 139.83(7), P(2)−Cu(2)−Re 143.79(4).

attached to the cluster surface via an Re−Cu bond and a B−H⇀Cu interaction, the latter involving a β-boron atom in the rhenium-ligating $\overline{\text{CB}\textit{B}\text{B}\textit{B}\text{B}}$ face. The Re−Cu distances (Re−Cu(1) is 2.7563(8) Å and Re−Cu(2) is 2.7866(7) Å) are significantly longer than the corresponding parameter (2.6583(6) Å) in the {Cu(PPh$_3$)} derivative of **1**,[2] while the B···Cu distances in **10a** (B(3)−Cu(1) is 2.095(5) Å and B(5)−Cu(2) is 2.096(6) Å) are rather shorter than the same separation (2.169(3) Å) in the related species. However, the geometry of the cluster is such that the two copper centers are too distant (∼4 Å) to form a Cu−Cu bond and the trimetallic unit instead is V-shaped, with the Cu(1)−Re−Cu(2) angle 93.89(2)°.

Both copper atoms in **10a** also lie rather close to B(4), with Cu(1)···B(4) being 2.355(6) Å and Cu(2)···B(4) 2.268(6) Å. A similar close contact (between platinum and boron) was found in the solid-state structure of **7a** described earlier that was relevant to the proposed behavior of that compound in solution. Likewise, the observed close Cu···B(4) approaches in molecules of **10a** may be related to fluxionality in solution, as discussed later (see Scheme 2). Alternatively, the proximity of the copper atoms to B(4) might simply be rationalized in terms of a tendency toward a tetrahedral coordination environment, as is often observed in copper−phosphine fragments bound to metallaheteroborane cluster surfaces.[23]

The molecular symmetry seen in the solid-state structure of **10a** is also evident in the solution NMR

Scheme 2. Alternative Structures for Compounds 10 and 11 in Solution

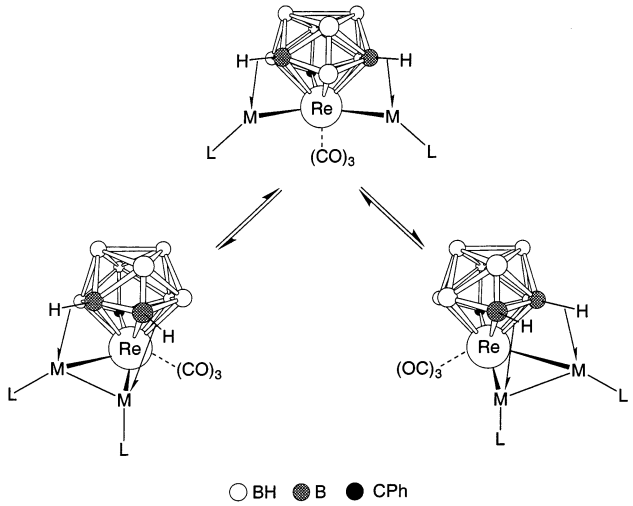

data of compounds **10** and **11** (Tables 2 and 3), with the peaks in their ^{11}B{^{1}H} NMR spectra having relative integrals 1:1:1:2:2:2 (**11a** has one coincidence). In each of the ^{13}C{^{1}H} NMR spectra the signals for the three rhenium-bound carbonyl ligands also show an apparent 1:2 intensity ratio, likewise consistent with mirror symmetry. All three compounds also display typical resonances in the aromatic regions of their ^{1}H and ^{13}C-{^{1}H} NMR spectra corresponding to their phenyl groups, with **10b** showing additional peaks at δ_H 2.34 (Me) and δ_C 118.9 (CN) and 3.2 (Me) for the coordinated NCMe ligand. However, as was the case with **5**−**7**, no signals are seen in the ^{1}H NMR spectra that may be attributed to protons involved in the B−H⇀M linkages (M = Cu, Au) in **10** and **11**. This feature is again presumably due to dynamic behavior of the exo-polyhedral fragment on the NMR time scale.[9] Although the Cu−Re−Cu unit in **10a** is shown not to be a closed triangle in the solid state, such an arrangement may occur during the fluxional behavior of all three compounds **10a**,**b** and **11** in solution. If one of the two exo-polyhedral {M−L} fragments occupies the γ-BH site during such a process while the other remains in an adjacent β site, the two may be in sufficiently close proximity that an M−M bonding interaction could temporarily form (Scheme 2). Indeed, the existence in solution of a species containing a carborane-supported ReM$_2$ (M = Cu or Au) triangle is not unreasonable, as structurally comparable M′$_3$−carbollide compounds are well established for M′ = Ru and Os.[24−27] Interconversion between the two Cu−Cu

(23) (a) Kang, H. C.; Do, Y.; Knobler, C. B.; Hawthorne, M. F. *Inorg. Chem.* **1988**, *27*, 1716. (b) Adams, K. J.; Cowie, J.; Henderson, S. G. D.; McCormick, G. J.; Welch, A. J. *J. Organomet. Chem.* **1994**, *481*, C9. (c) Thornton-Pett, M.; Kennedy, J. D.; Breen, S. P.; Spalding, T. R. *Acta Crystallogr.* **1995**, *C51*, 1496. (d) Batten, S. A.; Jeffrey, J. C.; Jones, P. L.; Mullica, D. F.; Rudd, M. D.; Sappenfield, E. L.; Stone, F. G. A.; Wolf, A. *Inorg. Chem.* **1997**, *36*, 2570. (e) Du, S.; Kautz, J. A.; McGrath, T. D.; Stone, F. G. A. *Dalton Trans.* **2003**, 46. (f) Kautz, J. A.; McGrath, T. D.; Stone, F. G. A. *Polyhedron* **2003**, 109. See also ref 9.

(24) Lebedev, V. N.; Mullica, D. F.; Sappenfield, E. L.; Stone, F. G. A. *Organometallics* **1996**, *15*, 1669.

(25) Lebedev, V. N.; Mullica, D. F.; Sappenfield, E. L.; Stone, F. G. A. *J. Organomet. Chem.* **1997**, *536*−*537*, 537.

(26) Ellis, D. D.; Franken, A.; Stone, F. G. A. *Organometallics* **1999**, *18*, 2362.

(27) Ellis, D. D.; Franken, A.; McGrath, T. D.; Stone, F. G. A. *J. Organomet. Chem.* **2000**, *614*−*615*, 208.

bonded species, as shown, would give rise to time-averaged mirror symmetry, as observed by NMR spectroscopy.

Conclusion

Our earlier work with the *closo*-icosahedral rhenacarborane tricarbonyl reagents **1** and **2** demonstrated that these salts would react with a variety of metal−ligand fragments, affording products in which these electrophilic groups become bonded in an exo-polyhedral manner to the {*closo*-3,1,2-$ReC_2B_9H_{11}$} and {*closo*-2,1-$ReCB_{10}H_{11}$} cage systems.[2,4,6,7,9] The present work significantly extends this chemistry to a reagent containing the new monocarbollide rhenium−tricarbonyl dianion [1,1,1-$(CO)_3$-2-Ph-*closo*-1,2-$ReCB_9H_9]^{2-}$ with 11 rather than 12 vertexes in the cage framework. Hence the new polymetallic compounds obtained have molecular structures hitherto not found in the metallacarborane field.[3] Clearly the study of reactions of the compounds **4** with other metal−ligand fragments merits examination, especially with the purpose of obtaining products in which the {*closo*-1,2-$ReCB_9$} moiety bridges two different metal systems as opposed to species such as **10** and **11**, where they are similar.

Experimental Section

General Considerations. All reactions were performed under an atmosphere of dry, oxygen-free dinitrogen using standard Schlenk-line techniques. Solvents were stored over and freshly distilled from appropriate drying agents prior to use. Petroleum ether here refers to that fraction of boiling point 40−60 °C. Chromatography columns (typically ca. 15 cm in length and ca. 2 cm in diameter) were packed with silica gel (Acros, 60−200 mesh). NMR spectra were recorded at the following frequencies: ^{1}H 360.1, ^{13}C 90.6, ^{11}B 115.5, and ^{31}P 145.8 MHz. The reagents [NEt_4][6-Ph-*nido*-6-CB_9H_{11}],[10−12] [$ReBr(CO)_5$],[28] [$Mn(NCMe)_3(CO)_3$][PF_6],[29] [$CuCl(PPh_3)$]$_4$,[30] and [$AuCl(PPh_3)$][31] were prepared by literature methods. The complexes [$PdCl_2$(dppe)], [$PtCl_2$(dppe)], and [$PtCl_2(PPh_3)_2$] were obtained by addition of the appropriate phosphine to a CH_2Cl_2 solution of [$MCl_2(NCPh)_2$] (M = Pd, Pt),[32] and [$NiCl_2$(dppe)] was formed from $NiCl_2$ and dppe in refluxing EtOH (15 min). All other materials were used as received.

Synthesis of the Salts [$N(PPh_3)_2]_{2-n}[NEt_4]_n$[1,1,1-$(CO)_3$-2-Ph-*closo*-1,2-$ReCB_9H_9$] (*n* = 0, 1). A THF (20 mL) solution of [NEt_4][6-Ph-*nido*-6-CB_9H_{11}] (0.41 g, 1.25 mmol) was cooled to −78 °C, and Bu^{n}Li (1.0 mL, 2.5 M solution in hexanes, 2.50 mmol) was added. After the mixture was allowed to warm to ca. −40 °C, a THF (20 mL) solution of [$ReBr(THF)_2(CO)_3$] (prepared by heating [$ReBr(CO)_5$] (0.50 g, 1.23 mmol) in refluxing THF (16 h)[13]) was introduced via a cannula. The solution was stirred for 4 h, [$N(PPh_3)_2$]Cl (1.40 g, 2.44 mmol) was added, and stirring continued overnight. Solvent volume was reduced to ca. 20 mL by evaporation in vacuo, giving a yellow precipitate that was isolated by filtration, washed several times with EtOH to remove excess [$N(PPh_3)_2$]Cl, and dried in vacuo to give a microcrystalline yellow solid (1.50 g). Integrated ^{1}H NMR spectroscopy showed this to be an approximately 1:1 mixture of the salts [$N(PPh_3)_2$][Y][1,1,1-$(CO)_3$-2-Ph-*closo*-1,2-$ReCB_9H_9$] (Y = NEt_4 (**4a**), $N(PPh_3)_2$ (**4b**)); complete metathesis could not be effected even with a vast excess of [$N(PPh_3)_2$]Cl. This mixture of salts **4a** and **4b**, referred to herein simply as compound **4**, was used without separation in subsequent syntheses. Crystalline samples of pure **4a** suitable for microanalysis and an X-ray diffraction study were obtained by fractional crystallization of the mixture (acetone−petroleum ether, −30 °C).

Reaction of [MCl_2(dppe)] (M = Ni, Pd, Pt; dppe = $Ph_2CH_2CH_2PPh_2$) and [$PtCl_2(PPh_3)_2$] with 4 in the Presence of Tl[PF_6]. (i) Compound **4** (0.15 g, 0.11 mmol), [$NiCl_2$(dppe)] (0.058 g, 0.11 mmol), and Tl[PF_6] (0.077 g, 0.22 mmol) were stirred in CH_2Cl_2 (20 mL) overnight. The reaction mixture was filtered through a Celite plug, concentrated, and transferred to the top of a chromatography column. A dark purple fraction was eluted with CH_2Cl_2−petroleum ether (2:1), which, after removal of solvent, yielded [1,3-{Ni(dppe)}-3-μ-H-1,1,1-$(CO)_3$-2-Ph-*closo*-1,2-$ReCB_9H_8$] (**5**) (0.036 g) as dark burgundy microcrystals.

(ii) Following the same procedure, compound **4** (0.20 g, 0.15 mmol), [$PdCl_2$(dppe)] (0.074 g, 0.13 mmol), and Tl[PF_6] (0.090 g, 0.26 mmol) gave [1,3-{Pd(dppe)}-3-μ-H-1,1,1-$(CO)_3$-2-Ph-*closo*-1,2-$ReCB_9H_8$] (**6**) (0.100 g) as purple microcrystals.

(iii) In a similar way, [1,3-{Pt(dppe)}-3-μ-H-1,1,1-$(CO)_3$-2-Ph-*closo*-1,2-$ReCB_9H_8$] (**7a**) (0.098 g) was obtained as orange-red crystals from the reaction of compound **4** (0.20 g, 0.15 mmol) with [$PtCl_2$(dppe)] (0.086 g, 0.13 mmol) and Tl[PF_6] (0.090 g, 0.26 mmol).

(iv) By an analogous procedure, the reaction of **4** (0.20 g, 0.15 mmol) with [$PtCl_2(PPh_3)_2$] (0.102 g, 0.13 mmol) and Tl[PF_6] (0.090 g, 0.26 mmol) afforded [1,3-{$Pt(PPh_3)_2$}-3-μ-H-1,1,1-$(CO)_3$-2-Ph-*closo*-1,2-$ReCB_9H_8$] (**7b**) (0.084 g) as an orange powder.

Synthesis of [$N(PPh_3)_2$][1,3,6-{$M(CO)_3$}-3,6-(μ-H)$_2$-1,1,1-$(CO)_3$-2-Ph-*closo*-1,2-$ReCB_9H_7$] (M = Re, Mn). (i) To a THF (10 mL) solution of [$ReBr(THF)_2(CO)_3$] (prepared as above from [$ReBr(CO)_5$] (0.10 g, 0.25 mmol)) was added a CH_2Cl_2 (20 mL) solution of compound **4** (0.30 g, 0.22 mmol) followed by Tl[PF_6] (0.10 g, 0.29 mmol). The reaction mixture was stirred overnight. After filtration through a Celite plug, solvent was removed in vacuo, and the residue was transferred to the top of a chromatography column. Elution with CH_2Cl_2−petroleum ether (3:1) afforded a yellow band, which was purified by further column chromatography using CH_2Cl_2−petroleum ether (2:1) as eluant to give yellow microcrystals of [$N(PPh_3)_2$]-[1,3,6-{$Re(CO)_3$}-3,6-(μ-H)$_2$-1,1,1-$(CO)_3$-2-Ph-*closo*-1,2-$ReCB_9H_7$] (**8**) (0.190 g) after removal of solvent in vacuo.

(ii) Compound **4** (0.20 g, 0.15 mmol) and [$Mn(NCMe)_3(CO)_3$]-[PF_6] (0.058 g, 0.14 mmol) were placed in a reaction tube, CH_2Cl_2 (20 mL) was added, and the mixture was stirred overnight to give a dark red solution. Solvent was removed in vacuo and the residue chromatographed. Elution with CH_2Cl_2−petroleum ether (3:1) removed a dark red band, from which [$N(PPh_3)_2$]-[1,3,6-{$Mn(CO)_3$}-3,6-(μ-H)$_2$-1,1,1-$(CO)_3$-2-Ph-*closo*-1,2-$ReCB_9H_7$] (**9**) (0.103 g) was obtained as a burgundy, crystalline solid after evaporation in vacuo.

Synthesis of [1,6-(ML)-1,7-(ML)-6,7-(μ-H)$_2$-1,1,1-$(CO)_3$-2-Ph-*closo*-1,2-$ReCB_9H_7$] (M = Cu, L = PPh_3 or NCMe; M = Au, L = PPh_3). (i) A mixture of **4** (0.20 g, 0.15 mmol), [$CuCl(PPh_3)$]$_4$ (0.094 g, 0.07 mmol), and Tl[PF_6] (0.091 mg, 0.26 mmol) was stirred overnight in CH_2Cl_2 (20 mL). After filtration through a Celite plug, the filtrate was concentrated by evaporation in vacuo and subjected to column chromatography. Elution with CH_2Cl_2−petroleum ether (2:1) removed a yellow band, from which [1,6-{$Cu(PPh_3)$}-1,7-{$Cu(PPh_3)$}-6,7-(μ-H)$_2$-1,1,1-$(CO)_3$-2-Ph-*closo*-1,2-$ReCB_9H_7$] (**10a**) (0.080 g) was isolated as a yellow crystalline solid.

(ii) Similarly, a mixture of compound **4** (0.30 g, 0.22 mmol) and [$Cu(NCMe)_4$][PF_6] (0.145 g, 0.39 mmol) in CH_2Cl_2 (30 mL) gave [1,6-{Cu(NCMe)}-1,7-{Cu(NCMe)}-6,7-(μ-H)$_2$-1,1,1-$(CO)_3$-

(28) Schmidt, S. P.; Trogler, W. C.; Basolo, F. *Inorg. Synth.* **1990**, *28*, 160.
(29) Reiman, R. H.; Singleton, E. *J. Chem. Soc., Dalton Trans.* **1974**, 808.
(30) Jardine, F. H.; Rule, J.; Vohra, G. A. *J. Chem. Soc. A* **1970**, 238.
(31) Bruce, M. I.; Nicholson, B. K.; Bin Shawkataly, O. *Inorg. Synth.* **1989**, *26*, 375.
(32) Anderson, G. K.; Lin, M. *Inorg. Synth.* **1990**, *28*, 61.

Table 4. Crystallographic Data for $4a\cdot{}^1/_8CH_2Cl_2$, $7a\cdot 2.5CH_2Cl_2$, and $10a\cdot CH_2Cl_2$

	4a·$^1/_8CH_2Cl_2$	**7a**·$2.5CH_2Cl_2$	**10a**·CH_2Cl_2
formula	$C_{54.13}H_{64.25}B_9Cl_{0.25}N_2O_3P_2Re$	$C_{38.50}H_{43}B_9Cl_5O_3P_2PtRe$	$C_{47}H_{46}B_9Cl_2Cu_2O_3P_2Re$
fw	1145.12	1271.50	1202.25
space group	$P2_1/n$	$P\bar{1}$	$P\bar{1}$
a, Å	11.5104(10)	10.8398(8)	9.4673(10)
b, Å	36.294(2)	11.6998(10)	13.685(2)
c, Å	13.8821(13)	20.239(2)	20.454(2)
α, deg		91.997(8)	96.4370(10)
β, deg	95.994(9)	95.733(6)	93.944(9)
γ, deg		112.855(7)	109.510(8)
V, Å^3	5767.7(8)	2345.8(3)	2466.1(5)
Z	4	2	2
ρ_{calc}, g cm^{-3}	1.319	1.800	1.619
μ(Mo Kα), mm^{-1}	2.216	5.946	3.517
wR_2, R_1 (all data)[a]	0.1197, 0.0866	0.0880, 0.0721	0.0830, 0.0454
wR_2, R_1 [$F_o > 4\sigma(F_o)$]	0.1033, 0.0485	0.0743, 0.0402	0.0741, 0.0328

[a] $wR_2 = [\sum\{w(F_o^2 - F_c^2)^2\}/\sum w(F_o^2)^2]^{1/2}$; $R_1 = \sum||F_o| - |F_c||/\sum|F_o|$.

2-Ph-*closo*-1,2-$ReCB_9H_7$] (**10b**) (0.025 g, 19%) as a yellow powder, the chromatographic purification using neat CH_2Cl_2 as eluant. IR (CH_2Cl_2): ν_{max}(CO) 2026 vs, 1961 s, 1912 s cm^{-1}.

(iii) By a procedure identical to that which afforded compound **10a**, but using [AuCl(PPh_3)] (0.064 g, 0.13 mmol) instead of $[CuCl(PPh_3)]_4$, the compound [1,6-{Au(PPh_3)}-1,7-{Au(PPh_3)}-6,7-(μ-H)$_2$-1,1,1-(CO)$_3$-2-Ph-*closo*-1,2-$ReCB_9H_7$] (**11**) (0.077 g) was isolated as yellow microcrystals.

X-ray Crystallographic Structure Determinations. Experimental data for compounds **4a**, **7a**, and **10a** are recorded in Table 4. Diffracted intensities were collected at 173(2) K on an Enraf-Nonius CAD4 diffractometer using graphite-monochromated Mo Kα X-radiation ($\lambda = 0.71073$ Å). Final unit cell dimensions were determined from the setting angles of 25 accurately centered reflections. Intensity data were corrected for Lorentz, polarization, and X-ray absorption effects, the last using a numerical method based on the measurement of crystal faces.

The structures were solved using conventional direct methods and refined by full-matrix least-squares on all F^2 data using SHELXTL version 5.03 and SHELXL-97.[33,34] All non-hydrogen atoms (with the exception of those in the solvate in **4a**) were assigned anisotropic displacement parameters. The locations of the cage carbon atoms were verified by examination of the appropriate internuclear distances and the magnitudes of their isotropic thermal displacement parameters. The hydrogen atoms involved in the agostic-type B−H⇀M interactions [H(4) in **7a** and H(3) and H(5) in **10a**] were located in difference Fourier syntheses; their positional parameters were refined with fixed isotropic thermal parameters [U_{iso}(H) = 1.2U_{iso}(parent)]. The remaining hydrogen atoms were included in calculated positions and set riding on their parent atoms with fixed isotropic thermal parameters [U_{iso}(H) = 1.2U_{iso}(parent), or U_{iso}(H) = 1.5U_{iso}(parent) for methyl hydrogens].

Compound **4a** cocrystallized with one-eighth molecule of CH_2Cl_2 per formula unit, which was located in general space but close to an inversion center (Wyckoff position *b*). The site occupancies of the carbon and chlorine atoms in the asymmetric fraction of the solvent molecule were assigned on the basis of a reasonable refinement of the thermal parameter of Cl(1), and these two atoms were then included in the refinement with equivalent isotropic thermal parameters. The chlorine atom Cl(1) was thus refined with a fixed site occupancy of 0.25, corresponding to one-eighth molecule per formula unit, and the carbon atom C(80) with a fixed occupancy of 0.125, as required by the site multiplicity. The C−Cl distances were restrained to reasonable values using the DFIX card.[34]

Each asymmetric unit in the crystals of **7a** contained one molecule of the compound plus two-and-a-half molecules of CH_2Cl_2 as solvate. Of these, one whole molecule was fully ordered and was freely refined with the hydrogen atoms riding on C(100) in calculated positions as above. The second whole CH_2Cl_2 molecule was disordered and treated as two fractional molecules with complementary occupancies that refined to an approximate ratio of 0.44:0.56. The carbon atoms C(200) and C(201) of the two fractions were located at the same site and with equivalent anisotropic thermal parameters; the corresponding C−Cl vectors of each fraction were at an angle of around 45° from each other. Hydrogen atoms in each fractional molecule were set riding on C(200) and C(201) as described above. The remaining half-molecule of solvate was located close to an inversion center (Wyckoff position *e*) and was refined with half-occupancy; the H atoms attached to the carbon atom C(300) were treated as indicated above. For the chlorine atoms attached to C(200), C(201), and C(300) the C−Cl distances were restrained to sensible values.

Compound **10a** cocrystallized with one molecule of dichloromethane in the asymmetric unit. The solvent molecule was fully ordered and refined without restraint; hydrogen atoms were included in calculated positions as before. Each of the phenyl rings of the PPh_3 ligand bound to Cu(1) was disordered, and thus each was treated as two separate parts with refining complementary occupancies. Thus, the two components of the ring C(11−16) had partial occupancies of approximately 0.51:0.49, as did those of the ring C(21−26); for the ring C(31−36) the ratio was 0.61:0.39.

Acknowledgment. We thank the Robert A. Welch Foundation for support (Grant AA-1201), and Dr. Andreas Franken for advice on the synthesis of [NEt_4][6-Ph-*nido*-6-CB_9H_{11}].

Supporting Information Available: Full details of the crystal structure analyses in CIF format. This material is available free of charge via the Internet at http://pubs.acs.org.

OM030122A

(33) *SHELXTL*, version 5.03; Bruker AXS: Madison, WI, 1995.
(34) Sheldrick, G. M. *SHELXL-97*; University of Göttingen: Göttingen, Germany, 1997.